EUR 243.e

EUROPEAN ATOMIC ENERGY COMMUNITY - EURATOM

SWELLING OF URANIUM

by

S. AMELINCKX - L. BINST-P. DELAVIGNETTE
J. NICASY (CEN) - E. RUEDL (EURATOM)

1963

EURATOM/United States Agreement for Cooperation
EURAEC Report No 371 established by CEN

Centre d'Etude de l'Energie Nucléaire - Mol, Belgium
under the Euratom Contract No 022-60-10 RDB

LEGAL NOTICE

This document was prepared under the sponsorship of the Commission of the European Atomic Energy Community (EURATOM) in pursuance of the joint programme laid down by the Agreement for Cooperation signed on 8 November 1958 between the Government of the United States of America and the European Atomic Energy Community.

It is specified that neither the Euratom Commission, nor the Government of the United States, their contractors or any person acting on their behalf:

1º — Makes any warranty or representation, express or implied, with respect to the accuracy, completeness, or usefulness of the information contained in this document, or that the use of any information, apparatus, method, or process disclosed in this document may not infringe privately owned rights; or

2º — Assumes any liability with respect to the use of, or for damages resulting from the use of any information, apparatus, method or process disclosed in this document.

This report can be obtained, at the price of Belgian Francs 60,—, from : PRESSES ACADEMIQUES EUROPEENNES - 98, Chaussée de Charleroi - Brussels 6.

Please remit payments :

— to BANQUE DE LA SOCIETE GENERALE (Agence Ma Campagne) - Brussels - account No 964.558,

— to BELGIAN AMERICAN BANK AND TRUST COMPANY - New York - account No 121.86,

— to LLOYDS BANK (Foreign) Ltd. - 10, Moorgate - London E.C.2,

giving the reference : ''EUR 243.e - Swelling of Uranium''.

Printed by CEN, Mol,
Brussels, September 1963.

EUR 243.e

SWELLING OF URANIUM by S. AMELINCK, L. BINST, P. DELAVIGNETTE, J. NICASY (CEN) and E. RUEDL (EURATOM)

European Atomic Energy Community - EURATOM
Euratom/United States Agreement for Cooperation
EURAEC Report No 371 established by CEN
Centre d'Etude de l'Energie Nucléaire, Mol (Belgium)
Euratom contract No 022-60-10 RDB
Brussels, September 1963 - pages 17 + figures 18.

This final report deals with some observations by means of transmission electron microscopy on dislocations in pure uranium, on a 1,5 % chromium-uranium alloy and on dislocations and radiation damage in platinum. These observations were performed as a preliminary study of the more complex behaviour of the fission product gases formed in uranium under irradiation. In order to get a better understanding of this behaviour it was first considered worth while to perform "Model-experiments" along the same line but on a metal of simpler crystal structure than uranium; this justifies the use of platinum. The platinum was in the form of thin beaten foils. Annealed, as well as annealed and subsequently fission fragment and α-particle irradiated foils were examined. The annealed foils show features which are typical for a face centered cubic

EUR 243.e

SWELLING OF URANIUM by S. AMELINCK, L. BINST, P. DELAVIGNETTE, J. NICASY (CEN) and E. RUEDL (EURATOM)

European Atomic Energy Community - EURATOM
Euratom/United States Agreement for Cooperation
EURAEC Report No 371 established by CEN
Centre d'Etude de l'Energie Nucléaire, Mol (Belgium)
Euratom contract No 022-60-10 RDB
Brussels, September 1963 - pages 17 + figures 18.

This final report deals with some observations by means of transmission electron microscopy on dislocations in pure uranium, on a 1,5 % chromium-uranium alloy and on dislocations and radiation damage in platinum. These observations were performed as a preliminary study of the more complex behaviour of the fission product gases formed in uranium under irradiation. In order to get a better understanding of this behaviour it was first considered worth while to perform "Model-experiments" along the same line but on a metal of simpler crystal structure than uranium; this justifies the use of platinum. The platinum was in the form of thin beaten foils. Annealed, as well as annealed and subsequently fission fragment and α-particle irradiated foils were examined. The annealed foils show features which are typical for a face centered cubic

EUR 243.e

SWELLING OF URANIUM by S. AMELINCK, L. BINST, P. DELAVIGNETTE, J. NICASY (CEN) and E. RUEDL (EURATOM)

European Atomic Energy Community - EURATOM
Euratom/United States Agreement for Cooperation
EURAEC Report No 371 established by CEN
Centre d'Etude de l'Energie Nucléaire, Mol (Belgium)
Euratom contract No 022-60-10 RDB
Brussels, September 1963 - pages 17 + figures 18.

This final report deals with some observations by means of transmission electron microscopy on dislocations in pure uranium, on a 1,5 % chromium-uranium alloy and on dislocations and radiation damage in platinum. These observations were performed as a preliminary study of the more complex behaviour of the fission product gases formed in uranium under irradiation. In order to get a better understanding of this behaviour it was first considered worth while to perform "Model-experiments" along the same line but on a metal of simpler crystal structure than uranium; this justifies the use of platinum. The platinum was in the form of thin beaten foils. Annealed, as well as annealed and subsequently fission fragment and α-particle irradiated foils were examined. The annealed foils show features which are typical for a face centered cubic

metal with a medium high stacking fault energy. Prismatic loops with a $\frac{a}{2}$ [110] Burgers vector result from the irradiation; this could be proved by observing their motion. The loops anneal out at the temperature where vacancies are thought to become mobile.

Preferential loop formation is noticed at certain boundaries, in particular along coherent twin boundaries. This is considered as evidence that correlated collision chains lead to preferential defect formation at these boundaries by "defocusing" of [110] focussons.

It is noticed that for small doses dislocation loops are not distributed at random in the interior of the grains but show a tendency to be aligned. This is interpreted as resulting of loop nucleation along the path of a fission fragment.

After quenching, specimens contain both cavities and loops. The damage rate of quenched specimens seems to be larger than that of annealed ones; the loop concentration is less along a denuded zone parallel to boundaries and subboundaries.

It is suggested that either the vacancy clusters left by quenching are nucleation sites for loops or that the vacancy clusters defocus focussons and hence increase the damage.

It is shown by means of contrast experiments that the loops left after irradiation are both interstitial and vacancy loops.

metal with a medium high stacking fault energy. Prismatic loops with a $\frac{a}{2}$ [110] Burgers vector result from the irradiation; this could be proved by observing their motion. The loops anneal out at the temperature where vacancies are thought to become mobile.

Preferential loop formation is noticed at certain boundaries, in particular along coherent twin boundaries. This is considered as evidence that correlated collision chains lead to preferential defect formation at these boundaries by "defocusing" of [110] focussons.

It is noticed that for small doses dislocation loops are not distributed at random in the interior of the grains but show a tendency to be aligned. This is interpreted as resulting of loop nucleation along the path of a fission fragment.

After quenching, specimens contain both cavities and loops. The damage rate of quenched specimens seems to be larger than that of annealed ones; the loop concentration is less along a denuded zone parallel to boundaries and subboundaries.

It is suggested that either the vacancy clusters left by quenching are nucleation sites for loops or that the vacancy clusters defocus focussons and hence increase the damage.

It is shown by means of contrast experiments that the loops left after irradiation are both interstitial and vacancy loops.

metal with a medium high stacking fault energy. Prismatic loops with a $\frac{a}{2}$ [110] Burgers vector result from the irradiation; this could be proved by observing their motion. The loops anneal out at the temperature where vacancies are thought to become mobile.

Preferential loop formation is noticed at certain boundaries, in particular along coherent twin boundaries. This is considered as evidence that correlated collision chains lead to preferential defect formation at these boundaries by "defocusing" of [110] focussons.

It is noticed that for small doses dislocation loops are not distributed at random in the interior of the grains but show a tendency to be aligned. This is interpreted as resulting of loop nucleation along the path of a fission fragment.

After quenching, specimens contain both cavities and loops. The damage rate of quenched specimens seems to be larger than that of annealed ones; the loop concentration is less along a denuded zone parallel to boundaries and subboundaries.

It is suggested that either the vacancy clusters left by quenching are nucleation sites for loops or that the vacancy clusters defocus focussons and hence increase the damage.

It is shown by means of contrast experiments that the loops left after irradiation are both interstitial and vacancy loops.

EUR 243.e

EUROPEAN ATOMIC ENERGY COMMUNITY - EURATOM

SWELLING OF URANIUM

by

S. AMELINCKX - L. BINST-P. DELAVIGNETTE
J. NICASY (CEN) - E. RUEDL (EURATOM)

1963

EURATOM/United States Agreement for Cooperation
EURAEC Report No 371 established by CEN

Centre d'Etude de l'Energie Nucléaire - Mol, Belgium
under the Euratom Contract No 022-60-10 RDB

CONTENTS

CAPTIONS FOR FIGURES

Fig. 1a : α-uranium foil after recrystallization at 650°C for 12 hours.
1b : Beaten platinum foil after recrystallization at 800°C for 2 hours.

Fig. 2a : α-uranium foil after mechanical deformation and partial annealing at 500°C for 2 hours. Dislocations in form of double lines.
2b : α-uranium foil after mechanical deformation and partial annealing at 500°C for 2 hours. Dislocations in strange contrast. Twin visible.

Fig. 3 : β-uranium foil with 1.5% chromium, quenched from 700°C and aged at 400°C for 1 hour.

Fig. 4 : Spherical cavities in quenched platinum foils. Interaction of the dislocations with the cavities in the middle of the segments marked C.

Fig. 5 : Dots and loops in fission fragment irradiated foils. By looking under a small angle along the photograph linear arrangements of dots will become apparent (dose 2.5×10^{11} fission fragments/cm^2)

Fig. 6 : Glide movement of loops under the influence of shear stresses set up by the electron irradiation. The arrows indicate loops in two different positions.

Fig. 7 : Preferential damage formation at coherent twin interfaces. Foil plane is (110). Foils irradiated with fission fragments (dose 2.5×10^{11} fission fragments/cm^2).

Fig. 8 : Schematic view of atomic arrangement at a coherent twin boundary in a face centered cubic crystal. The arrangement is viewed along the $\langle 1\bar{1}0 \rangle$ direction. It is clear that a collision chain propagating along 1 - 2 - 3 will result in the displacement of atoms 4 and 5 and possibly other atoms.

Fig. 9 : Platinum foil after different irradiation treatments.
a) After irradiation by 10^{18} n/cm^2 at -180°C. Observed at room temperature.
b) After irradiation by 7×10^{15} n/cm^2 in contact with uranium at 80°C. Raggy dislocations marked by arrow.

Fig. 10 : Platinum foils exposed to α-particles by irradiating with neutrons in contact with boron nitride during 10 days at a flux of 1.4×10^{12} thermal neutrons/cm^2 sec. During irradiation the foil was kept at liquid nitrogen temperature but the observations were made at microscope temperature. No denuded zone is found along the boundary.

Fig. 11 a) Polyhedral cavities formed on pulse annealing in the microscope of α-irradiated specimens.
b) On repeated pulse annealing some cavities disappear, others start producing dislocation loops. Notice also pairs of dots presumably resulting from loops intersecting the surfaces.

Fig. 12 : Well developed polygonal loops in specimen heavily irradiated with α-particles (same dose as Fig. 10). The specimen was annealed during 1 hour at 500°C. Notice the separation into families of loops having the same outline and the same contrast. Some loops are out of contrast satisfying the criterium $\bar{g}.\bar{b} = o$ ($\bar{g}$ = diffraction vector) ; they only show residual contrast due to the radial displacements . The diffraction vector is indicated. Some of the out of contrast loops have a size comparable to the foil thickness suggesting that they are nearly in the foil plane.

Fig. 13 Prismatic loops in the f.c.c. structure, showing the glide cylinder on as dotted lines. The direction of climb is indicated by arrows.
a) Vacancy loops
b) Interstitial loops

Fig. 14 Interstitial and vacancy loops in normal and inclined position ; c and a denote respectively clockwise and anti-clockwise rotation of the lattice.
a) Vacancy loop normal to the beam
b) Vacancy loop inclined
c) Interstitial loop normal to the beam
d) Interstitial loop inclined.

Fig. 15 : Relative position of diffraction spot and corresponding Kikuchi line allowing the determination of the sign of s and S.
a) $s = o$ b) $s > o$ c) $s < o$
S is the sense in which the lattice has to be rotated in order to go into the Bragg condition.

Fig. 16 Sequence of photographs illustrating the procedure used in determining the character of one family of loops indicated by arrows. The corresponding diffraction patterns in their correct orientation with respect to the images are also shown.
a) Foils normal to the beam : foil plane is (110), operating reflection ($\bar{1}11$). Loops showing residual contrast are indicated by arrows.
b) Foil is inclined 45° with respect to the incident beam. The axis of rotation is horizontal on the photograph, the sense of inclination is indicated by up and down. Operating reflection ($\bar{2}02$) $s > o$.
c) Same as (b). Operating reflection ($20\bar{2}$), $s > o$.

Fig. 17 : Sequence of photographs used to determine the characters for a number of loops similar to that shown in Fig. 16 . The deduced character is indicated for a number of loops.

Fig. 18 Removal of the stacking fault of the interstitial loop by glide of partials along the loop plane.
a) The interstitials form a disc
b) A partial passes above the plane of the loop
c) A second partial passes underneath the loop.

SWELLING OF URANIUM

SUMMARY

This final report deals with some observations by means of transmission electron microscopy on dislocations in pure uranium, on a 1.5 % chromium-uranium alloy and on dislocations and radiation damage in platinum. These observations were performed as a preliminary study of the more complex behaviour of the fission product gases formed in uranium under irradiation. In order to get a better understanding of this behaviour it was first considered worth while to perform "Model experiments" along the same line but on a metal of simpler crystal structure than uranium ; this justifies the use of platinum. The platinum was in the form of thin beaten foils. Annealed, as well as annealed and subsequently fission fragment and α-particle irradiated foils were examined. The annealed foils show features which are typical for a face centered cubic metal with a medium high stacking fault energy. Prismatic loops with an $\frac{a}{2}$ [110] Burgers vector result from the irradiation ; this could be proved by observing their motion. The loops anneal out at the temperature where vacancies are thought to become mobile.

Preferential loop formation is noticed at certain boundaries, in particular along coherent twin boundaries. This is considered as evidence that correlated collision chains lead to preferential defect formation at these boundaries by "defocusing" of [110] focussons.

It is noticed that for small doses dislocation loops are not distributed at random in the interior of the grains but show a tendency to be aligned. This is interpreted as resulting of loop nucleation along the path of a fission fragment.

After quenching, specimens contain both cavities and loops. The damage rate of quenched specimens seems to be larger than that of annealed ones ; the loop concentration is less along a denuded zone parallel to boundaries and subboundaries.

It is suggested that either the vacancy clusters left by quenching are nucleation sites for loops or that the vacancy clusters defocus focussons and hence increase the damage.

It is shown by means of contrast experiments that the loops left after irradiation are both interstitial and vacancy loops.

INTRODUCTION

Swelling of uranium is of particular interest since it imposes limits to an obtainable burnup and on the fuel operating temperature. The volume increase is attributed to segregation of the gaseous fission products in bubbles within the fuel. A number of factors are known or suspected to influence the swelling behaviour. Structural and irradiation variables and a number of phenomena are involved. A lot of theoretical and experimental work has been done on the study of these phenomena.

It appears that the scale of bubble nucleation and growth may be of considerable importance. Cases where unacceptable swelling behaviour occurs are due to formation of bubbles of $\geq 10^{-4}$ cm size. This occurs if samples are thermally cycled during irradiation or alloying additions are present. More recent experiments on α-uranium irradiated at constant temperatures between 200° and 600°C, have shown gas bubble formation on a much finer scale. α-uranium irradiated under such conditions after 0.5 % burnup contains bubbles of $\sim 10^{-5}$ cm diameter at a spacing of 5×10^{-5} cm. A remedy to excessive swelling would then consist in finely dispersing the gas bubbles.

The fine scale bubble formation has been considered from a theoretical point of view by GREENWOOD et al. [1]. These authors point out that the nucleation of gas bubbles and surface tension forces which exert a strong restraint on the bubble growth are rate controlling in the swelling phenomena. There are indications in other systems [24] that the gas bubbles nucleate under certain circumstances on dislocations, preferentially on node points of the dislocation networks [25]. It was even found, that, if small enough, the bubbles can be used as a convenient decoration procedure [26] for revealing dislocations. If this is true it would be necessary to introduce a large number of nucleation sites in order to get a fine dispersion of gas bubbles. This could e.g. be done by heavy plastic deformation.

1. SUBJECT OF THE PRESENT RESEARCH

The aim of this research was to establish whether bubbles of inert gas formed during irradiation in uranium are nucleated at dislocations or whether some alternative nucleation mechanism is operative e.g. nucleation at small precipitate particles. Particularly we intended to consider in some detail and from a fundamental point of view the following problems :

1) the dislocation configuration of uranium
2) the nature of the nucleation sites of the bubbles
3) the mechanism of growth of the bubbles
4) the growth kinetics of the bubbles
5) the influence of thermal cycling
6) the effect of pre-irradiation heat treatment.

Since transmission electron microscopy has proved to be an exceptional tool in studying dislocations, precipitates or radiation damage, this technique has been mainly used for the present research.

In order to get a better understanding of the phenomena to be investigated it was first necessary to perform "Model experiments" on the same line on a metal of simpler crystal structure than uranium. Platinum was the obvious choice because it is an attractive metal in many respects.
Its atomic number is comparable to uranium, it has good surface properties and does not become very active on irradiation. As a consequence of its high melting point it was hoped that irradiation damage would not anneal out completely at reactor temperature and this proved correct. Furthermore, although most of the face centered metals have been studied intensively by transmission electron microscopy, not much attention has been devoted to platinum.

This final report consists of two parts : the first part is concerned with a description of the results on uranium, the second part contains the summary of the results on the "Model experiments" on platinum.

2. EXPERIMENTAL METHODS

The method used was transmission electron microscopy of thin foils.

a) Thinning of bulk specimens

Suitable techniques of thinning as deformation and/or electropolishing were explored.

b) Method of observation

The technique of examining the thin foils referred to here has been developed in recent years [2]. The contrast observed in these foils is mainly diffraction contrast. It requires careful orientation and therefore the possibility to give a wide range of orientations to the specimen. Combining the techniques of observation in transmission and of selected area diffraction, direction and sense of Burgers vectors of dislocations can be determined. This information is of importance in view of the rôle of dislocations in the nucleation and growth process of the bubbles.

c) Equipment

The electron microscope used in this study was a Siemens Elmiskop I.

3. URANIUM

3.1. Material

Uranium with different amounts of impurities was used. The material consisted of :

a) vacuum melted zone refined uranium of the following impurity content : carbon 60 ppm ; iron 23 ppm ; aluminium 29 ppm ; titanium 16 ppm.

b) uranium of reactor grade purity

c) uranium with 1.5 % chromium.

3.2. Preparation of thin foils

The procedure for preparation of thin uranium foils of large homogeneous grain size and smooth clean surfaces was somewhat the same as described by FISHER [3]. This method consists of obtaining large α-uranium single crystals by a grain coarsening method. Grain coarsening implies a discontinuous type of grain growth during which a few grains grow to a large size in a fine-grained matrix. This can be achieved by a dispersion of inclusions (of impurities originally present) on a very fine scale in the matrix. These inclusions are very effective for inhibiting continuous growth. During prolonged annealing the impurities coalesce or dissolve in the matrix and some grains begin abruptly to grow at the expense of the fine grains.

The uranium foils of 200 micron thickness were first sealed into evacuated quartz capsules for γ-phase heat treatment. The capsules were heated in a furnace at 1000°C for several hours and then quenched in a water bath in order to disperse the impurities. The foils were then reduced in thickness to about 30 microns by alternated rolling and annealing and were finally annealed at 650°C during several hours. Surface oxides were removed by electropolishing.

In order to introduce dislocations after recrystallization the foils of α-uranium were deformed by rolling or by rapidly cooling and were afterwards annealed at temperatures between 400° and 600°C. The foils with 1.5 % chromium content were quenched from 750°C in order to retain the β-phase.

3.3. Electropolishing procedure

Numerous solutions have been examined as possible electrolytes. The technique which gave satisfactory results [4] was the following :

a) The foils are rapidly thinned in an electrolyte consisting of 80 % orthophosphoric acid, at 6 volts using uranium as cathode.

b) Final polishing in a solution of 75 % sulfuric acid, 18 % glycerol, and 7 % water at 6 volts with platinum as cathode. A thin passivating layer is formed by this treatment which prevents the specimen from stronger oxidation. The specimens are withdrawn from the solution and washed in ethyl alcohol.

It was found that uranium foils were easier to polish if the impurity content was low. Uranium foils with 1.5 % chromium were sometimes preferentially attacked.

3.4. Observation in the microscope

The examination of the recrystallized foils revealed a rather homogeneous grain size of 50 microns or more. A surface structure was always visible on the micrographs. This is shown in Fig. 1,a which represents a typical region of recrystallized foil. For comparison see Fig. 1,b which represents an annealed beaten platinum foil. Only few irregular dislocation segments and twins were present in the α-uranium foils. Slip traces were sometimes visible.

Foils deformed and partially annealed prior to examination reveal many dislocation segments and twins. Figs. 2,a,b show typical regions of a deformed specimen. The dislocations are found to be preferentially in form of double lines. Sometimes this was due to two operating reflections, but in other cases not. It is therefore assumed that the dislocations are split in partials. Small defects as inclusions or dislocation loops are rather difficult to distinguish from the surface structure left after polishing as shown in Fig. 1,a and Fig. 2.

Foils with 1.5 % chromium were quenched, from 700°C in order to retain the β-phase. This could be proved by electron diffraction. Fig. 3 represents a micrograph of a β-uranium foil. The features visible on this photograph are not well understood.
Some contrast effects are presumably due to dislocations. It is assumed that the strips, also visible in Fig. 3, represent regions of transformation of the metastable β-phase to α-uranium.

3.5. Conclusions

The direct observation of uranium foils by transmission electron microscopy has supplied qualitative information on dislocations. The following conclusions are drawn as a result of the observations.

a) Thin uranium foils of large homogeneous grain size prepared in a way somewhat similar as described by FISHER prove to be a suitable starting material for radiation damage studies by electron microscopy.

b) The electropolishing technique for obtaining very thin regions is still unsatisfactory. A slight surface structure is always left after electropolishing. We were able to observe the dislocation structure in the foils. However, small defects as inclusions or dislocation loops were rather difficult to recognize.

c) It is assumed that the dislocations in α-uranium are split in partials. Based on this observation the following recommendations for future work are advanced.
Better electropolishing conditions should be explored in order to obtain passivated surfaces without surface structure. Attempts should be made to generate dislocation networks after deformation and partial annealing. Examination of networks should help to clarify whether the dislocations are split in partials.

4. PLATINUM

This part is concerned with a study of the substructure of the platinum foils prior to irradiation, as well as after neutron, α-particle and fission-fragment damage.

4.1. Foil preparation and irradiation technique

The platinum used in these investigations was in the form of beaten foils having a thickness of about one tenth of a micron. Its purity was about 99.998 %. The foils were thin enough to transmit electrons as received, but heavily deformed. They were therefore annealed for about one hour at 800°C. They generally exhibited

a pronounced (110) recrystallization texture. Coherent twin boundaries perpendicular to the foil plane were not uncommon. Quenching of these foils was performed either in air or in vacuum by suddenly switching off the electrical current being used for heating.

For the neutron irradiation the foils were capsuled in evacuated quartz tubes and irradiated at about -180°C up to a dose of 10^{18} n/cm^2 in a liquid nitrogen facility in the BRI reactor. The specimens were subsequently observed at room temperature. The irradiation with fission fragments was performed in evacuated quartz by irradiating stacks of platinum foils in contact with a uranium foil. The sandwiches were then irradiated in the BRI reactor at reactor temperature (80°C). For the α-particle bombardment, stacks of foils were packed in contact with boron nitride and irradiated in the BRI reactor. The irradiation was performed both at liquid nitrogen temperature and at room temperature.

4.2. Results of observation

4.2.1. Annealed specimens

The dislocations in platinum appear as single lines at the resolution available with the Siemens Elmiskop I (operated at 100 kV).

However, there are indirect indications that the dislocations are dissociated ; we noticed configurations as observed previously by WHELAN in stainless steel and interpreted by this author as Lomer-Cottrell barriers [5].

The observation of piled-up dislocations is another indication in the same way. Furthermore, cross slip has been observed only exceptionally and it occurred in a rather complicated way. Finally, annealing twins were rather common. All these observations strongly suggest a definite separation into partials. No extended or contracted nodes are resolved in hexagonal networks, showing that the stacking fault energy must be large enough to cause a separation inferior to the resolving power of the microscope. This puts a lower limit to the value of γ of about 30 erg/cm^2.

4.2.2. Quenching experiments

Quenching experiments in metals have shown that vacancies precipitate either as loops [6] or as tetrahedra [7] depending on the magnitude of the stacking fault energy. No direct observations of quenched-in defects are available for platinum.

The very thin foils described above, were quenched after annealing in vacuum at a temperature just below the melting point. After some annealing most of the quenched foils present ring-shaped circular features, sometimes polygonal features of varying size, but mostly smaller than 100 Å (see Fig. 4). The contrast is quite different from that of dislocation loops. It is difficult to

decide whether the features are at the surface or in the interior. Some of the larger features seem to be at the surface since in one of them moiré fringes could be observed. After cleaning with different acids most of the features remain however. It is believed that they are in the interior of the foil. Many dislocations connecting top and bottom surface interact strongly with the rings somewhere in the middle of the segments ; see e.g. the segments marked C. The projected length of the segments is about 1000 Å, and since the thickness of the foil is about the same (as derived from slip traces) the inclination of the segments is about 45°. It is unlikely that a surface feature would strongly interact with a dislocation line 500 Å below it without changing considerably the shape at the same time. It is therefore thought that the circular features are inside the foils. Since they are **always** observed as **circular** it is suggested that they are in fact spherical voids or cavities and **not** loops.

The voids are preferentially located on dislocations, presumably because the latter were stopped on passing close to the void. It is unlikely, although not excluded, that voids were nucleated on dislocations. The cavities formed in the quenched foils are difficult to eliminate ; they appear to be stable up to about 800°C. They grow slightly after annealing at about 500°C and disappear after annealing at about 800°C.

The question now arises why vacancies in platinum prefer to form voids instead of loops. According to FRANK [8] the energy of a spherical void is lower than that of the dislocation loop for small n (n : number of vacancies in the aggregate). Initially vacancies will form spherical voids. For n larger than some critical value, however, the loop has the smaller energy and one would therefore expect that the final defect will generally be a loop. However, in going from the spherical shape to the dislocation loop the void has to increase its surface considerably and adopt presumably a complicated intermediate shape. An energy barrier has to be overcome for the loop to form and this energy is directly proportional to the surface energy. Since platinum is one of the metals with the highest surface energy, the spherical cavities may find it difficult to transform into loops.

4.2.3. Irradiated material

4.2.3.1. Radiation damage induced by fission fragments

The results of fission fragment damage in platinum appear to be rather similar in aspect to the results of neutron damage in copper presented by SILCOX and HIRSCH [9]. The main difference is that similar concentrations of defects are obtained after a much shorter irradiation time owing to the much higher energy of fission fragments.

a) **Damage within the grain**

The damage consists of black dots and dislocation loops. A clear distinction between dots and loops as was made in the case of copper by MAZEY and

BARNES [10] is not possible here. The black dots may well be of the same nature as the resolvable loops, only much smaller.

(i) The contration increases with dose, but the dependence is less than linear. Foils which have been bombarded respectively with 2.5×10^{10} and 2.5×10^{11} fission fragments/cm^2 present about 5×10^{10} and 1.5×10^{11} dots/cm^2. Considering a foil thickness of 1000 Å, the total number of dots per unit volume is 5×10^{15} and 1.5×10^{16}. With increasing dose the concentration of loops of all sizes increases. In particular, loops of larger size start to appear, presumably as a result of growth and coalescence of smaller loops (Fig. 5).

(ii) It was found that even in uniformly irradiated specimens the dots are not arranged at random but on the contrary show a preference to be on straight lines in certain areas [11]. This is shown in Fig. 5 where the linear arrangements are indicated by arrows. As described later, spots line up along grain boundaries and more specially along twin boundaries. This effect is, however, completely different from the phenomenon discussed here, which takes place within the bulk of the grains.
A statistical analysis shows that the probability, that the linear arrangement should be fortuitous, is small. It is therefore suggested that they result from the passage of a fission fragment at very small angles of incidence with the foil. The dots or loops are presumably nucleated at spots where primary knock-ons have taken place, resulting in the displacement cascades as suggested by SILCOX and HIRSCH [9]. The dots would then represent vacancy loops.

(iii) In general there is no denuded zone along the grain boundaries in foils annealed prior to irradiation, hereby suggesting that long range diffusion during irradiation is not important for the formation of loops. In copper, on the contrary, zones denuded of loops but not of dots were usually found [11] along the grain boundaries. This is in fact one of the arguments that was used to conclude to the existence of two kinds of defects clusters.

(iv) A most remarkable phenomenon was noticed. In a number of cases loops started to oscillate slowly in a jerky fashion between two positions, as shown in Fig. 6, thereby changing shape. The movement is conservative since the loop has again the same size when returning to its original position. The direction of movement is along <110>. The observation proves unambiguously that the loops are of prismatic character since they can glide on a cylinder parallel to <110>. The possibility of glide excludes the presence of a stacking fault within the loop. Movement of the same type has been described previously by PASHLEY in gold films [13].

(v) Annealing at temperatures in the range of 420–470°C causes a decrease in the number of dots and a slight increase in size. The temperature of 420°C corresponds to the range where according to PERCY [12] vacancies become mobile. In this temperature range rapid polygonization is observed in quenched specimens. It is therefore reasonable to associate the arrangement of dots with the movement of vacancies resulting in the growth of the larger loops at the expense of the smaller ones. At 470°C the dots completely disappear after a 1/2 hour annealing and the foil becomes clear as before.

b) Preferential damage formation at coherent twin boundaries

In the course of these investigations it was found that dots are preferentially formed at coherent twin boundaries. This is pronounced in foils irradiated to an intermediate dose (2.5×10^{11} cm^{-2}) as shown in Fig. 7. We believe that this phenomenon gives rather strong evidence that focusing collisions take place in platinum and contribute to the dot formation. The transport of defects could for instance take place by means of focusing collision chains, either of the SILSBEE type [14] or of the type discussed more recently by LEHMANN and LEIBFRIED [15].

(i) In the face centered cubic lattice focusing of the SILSBEE type [14] proceeds mainly along <110> directions. To a smaller extent focusing also occurs along <100> and <111> directions. This was shown experimentally by THOMPSON [16] by means of sputtering experiments and it results from the machine calculations of VINEYARD [17] and from theoretical calculations by LEHMANN and LEIBFRIED [15].
Let us consider as a specific example a focusing chain along the <110> direction. The <110> direction in one crystal of the twin is parallel to a <114> direction in the other crystal. On arriving at the twin interface the focusing collision will suddenly become a non-focusing one or in other words a defect producing collision, provided enough energy is left to cause the displacement. This is shown schematically in Fig. 8.
Focusing collision chains are expected to be defocused by isolated point defects. In an attempt to demonstrate this we intensively studied quenched foils; so far no preferential defect formation at coherent twin boundaries was found.

(ii) The second type of focusing mechanism consists in the propagation of atoms along the open <110> and <100> channels in the face centered cubic structure. The atoms, shot out from a displacement spike, now travel along the open tunnels. On arriving at the twin boundary the tunnel changes abruptly its direction (see Fig. 8), the atom "hits the wall of the tunnel" and therefore damage production takes place. This second type of focusing has a larger range and moreover takes place at higher energies than the SILSBEE

mechanism . The observed decoration effect is probably the result of both processes . The decoration observed at isolated dislocations can also be explained as the result of defocusing of collision chains passing close to a dislocation . The curvature of the lattice rows in the vicinity of the dislocation may be sufficient to enhance locally the damage rate and hence increase the local nucleation rate of the loops .

Summarizing, the coherent twin interface plays a unique role in causing damage because it is an effective barrier for focussons without being a sink for the defects formed in its vicinity . Focussons, which in the perfect crystal would dissipate their energy without causing displacement, will do so on intersecting a twin interface .

4.2.3.2. Effect of quenching

Quenched and unquenched foils were irradiated in contact with the same uranium foils, i.e. under exactly the same circumstances . The following observations were made :

(i) the loop concentration in the quenched foils is larger than in the unquenched ones

(ii) in the quenched foils denuded zones are formed along the boundaries on irradiation .

These observations can be explained either as the result of enhanced damage formation due to the presence of vacancies and vacancy clusters (e.g. by defocusing of collision chains), or as the result of enhanced nucleation [11] .

In quenched foils the boundaries are bordered by zones containing less vacancies . The formation of denuded zones on irradiation is as a consequence a confirmation of the first observation .

4.2.3.3. Radiation damage induced by neutron irradiation

Foils which have been irradiated in the reactor for 14 days at liquid nitrogen temperature (10^{18} n/cm^2) were investigated in the electron microscope at room temperature . Fig. 9 shows a photograph which represents an area bombarded by neutrons alone . When comparing Fig. 9a with Fig. 9b which represents another region which was in contact with uranium during neutron irradiation, one difference is obvious . The measles effect in the form of black dots is only visible in foils exposed to fission fragments . However, both photographs show defect formation at subboundaries and raggy-shaped dislocations (arrow) . This suggests that damage also occurs in the neutron irradiated foils . The fact that no loops were nucleated within the grains is probably due to the low instantaneous concentration of defects . At heterogeneities such as dislocations and subboundaries, a high concentration of defects builds up locally and this results in the decoration effect . This observation points to preferential damage formation and heterogeneous nucleation especially under conditions of small instantaneous concentration .

4.2.3.4. α-damage

A stack of platinum foils was exposed to α-particles from boron nitride in contact with it during 10 days (neutron flux of 10^{12} n/cm/sec) at liquid nitrogen temperature. The foils in direct contact with the boron nitride were discarded ; no attempt was made to evaluate the exact α-dose in the examined foils.

After irradiation the foils were threaded by a large concentration of dislocations segments and a high concentration of small dislocation loops is also present (see Fig. 10). The annealing behaviour of these foils is more complex than that of the fission fragment irradiated ones. This is probably a consequence of the presence of helium atoms which become mobile in roughly the same temperature range where annealing of defects takes place.

On pulse annealing in the microscope by increasing the electron beam intensity, small polyhedral cavities are formed ; some loops are left. On repeated pulsing some of the cavities apparently produce new loops, as for instance in Fig. 11 a,b.

The temperature of the specimen during these pulses is not known. Therefore experiments were also performed with the specimens heat treated in a furnace. Annealing at 500°C during 1 hour gives rise to large polygonal loops, of which examples are shown in Fig. 12. The nature of the loops is discussed below. Annealing at 500°C during a 1/2 hour introduced cavities rather similar to those obtained by pulse annealing ; the concentration was however smaller. These cavities appear to be stable up to 700°C.

Tentatively, the annealing behaviour can be understood by assuming that the dissolved helium becomes mobile at about 560°C, i.e. just above the temperature where defects become mobile, i.e. 500°C. Annealing at the lower temperature (500°C) would make possible the migration of the radiation produced defects and the formation of loops ; the helium would remain dispersed. At the higher temperature the helium may become sufficiently mobile to agglomerate and form cavities, whereas loops anneal out, the vacancies being absorbed by the cavities.

The formation of the cavities during pulse annealing in the microscope may be due to the high instantaneous concentration of vacancies. The treatment would therefore be somewhat comparable to a quench, the presence of the helium may stabilize the cavities and make them grow by attracting vacancies.

4.3. Determination of the loop character

Making use of the one-sided nature of dislocation contrast when the interference error is appreciably different from zero, it is possible to determine the sign of the Burgers vector. Hence, it becomes also possible to determine the character of the prismatic loops, i.e. whether they are due to vacancies or inter-

stitials, at least provided the loops are not too small. The method has been applied to prismatic loops in deformed magnesium oxide [18] and to glissile dislocations parallel to the foil plane in tin disulfide [19]. In the platinum specimens irradiated by α-particles at liquid nitrogen temperature, the loops can be made to grow to a sufficient size by annealing around 500°C during 1 or 2 hours. We shall discuss contrast experiments with loops which lead to the conclusion that both types of loops occur.

4.3.1. Burgers vector of the loops

The direction of the Burgers vector is not required for a determination of the loop character, however, it is helpful in finding the loop plane. In the f.c.c. metals, prismatic loops have Burgers vector of the type $\frac{a}{2}$ [110] as shown by HIRSCH et al. [6] for vacancy loops in quenched aluminium. For the loops in α-irradiated and annealed platinum the Burgers vector could be inferred from the following observations.

(i) Residual contrast is observed for reflections of the type {111}, {311}, {100} (Fig. 12). Although these extinctions were observed in different specimens, they are all consistent with an $\frac{a}{2}$ [110] type vector. Other vectors consistent with this combination of three would have higher indices and are therefore improbable.

(ii) Occasionally some of the smaller loops oscillate during observation. Their direction of movement is consistent with an $\frac{a}{2}$ [110] type Burgers vector, if it is assumed that they are prismatic loops moving conservatively on their glide cylinder (Fig. 6).

4.3.2. Loop plane

When observing the loop shapes in annealed foils it is evident that they can be divided into categories having the same outline and the same contrast. We assume that they are located in the same plane and that their Burgers vectors have the same direction. In certain orientations the loops appear as small segments because the loop plane is parallel to the incident beam. It is then found that the loops lie preferentially in (110) planes at least after annealing, they apparently have a tendency to become purely prismatic. This tendency is explained as follows :

(i) Conservative glide on a prismatic surface defined by the loop and of which the direction is parallel to $\bar{b}$, may reduce the loop length. This length is a minimum if the loop plane is perpendicular to $\bar{b}$. In this glide process segments of mixed character become pure edges, and hence their energy per unit length increases. However, the decrease in length overcompensates this increase if Poisson's ratio is not too large.

(ii) When growing by climb the loops are induced to rotate around an axis in their plane, towards the purely prismatic orientation. This is true as well for vacancy loops as for interstitial loops, as shown in Fig. 13 where the arrows indicate the sense of climb, giving rise to loop growth.

From these arguments it becomes plausible to assume that most of the larger loops will be in the (110) plane perpendicular to their Burgers vector or very nearly so.

4.3.3. The sign of the Burgers vector - Principle of the method

The sign of the Burgers vector can be determined if the loop plane is put at an angle with respect to the electron beam. This situation is represented in Fig. 14.

The sign of s, the excitation error, follows from the relative position of the spot, responsible for contrast, and the Kikuchi lines associated with it. For a spot to the right of the tilt axis the sign can be deduced from Fig. 15 and mutatis mutandis if it is to the left of the tilt axis. The sign of s is called conventionally positive if the reciprocal lattice point is inside Ewald's sphere. The sign of $\bar{s}$ determines the sense $\bar{S}$ into which the lattice has to be rotated in order to approach the Bragg condition; $\bar{S}$ is indicated in Fig. 15.

4.4. Illustration of the procedure as applied to the loops in platinum

The whole procedure shall now be followed step by step for one family of loops.

4.4.1. Observation in the normal position of the foil

(i) *Burgers vector*:

Fig. 16 shows a number of loops of which some, indicated by arrows, only exhibit so-called residual contrast, due to the radial displacements. The foil plane is (110), the contrast producing spot is $(\bar{1}11)$. From the three $\frac{a}{2}\langle 110\rangle$ type vectors in the $(\bar{1}11)$ plane, one is perpendicular to the foil plane $\frac{a}{2}\langle 110\rangle$. The others form an angle of 30° with the plane and would correspond either to very inclined prismatic loops, or to loops which are far from being purely prismatic. The loops are furthermore out of contrast for other reflections normally operating in this orientation. It is therefore concluded that the Burgers vector of the indicated loops must be $\frac{a}{2}\langle 110\rangle$ i.e. perpendicular to the foil plane.

(ii) *Loop plane*:

When having a vector perpendicular to the foil plane the loop must lie very nearly in the foil plane in order to be purely prismatic. This is in agree-

ment with their shape which suggests that they are not in very inclined planes. This conclusion can be checked further by looking at it in the inclined positions. The procedure is furthermore not dependent on small deviations from the assumed loop plane. In this case an uncertainty of about 20° each way in the inclination with respect to the foil plane would not alter the final conclusions.

4.4.2. Observations in the inclined positions of the foil

(i) *Rotation axis and tilt axis*

The foil is mounted on a wedge, in the way described by GROVES and KELLY [12]. The foil is now inclined at about 45° with respect to its normal position and we know in which sense. The axis of rotation is taken parallel to the tilt axis of the specimen holder. Its exact direction is deduced by measuring a number of distances between the same loop pairs on photographs taken in both positions. The ratios of the distances in the inclined position to the corresponding distances in the normal position have a maximum for the direction of the axis of rotation and a minimum for the direction perpendicular to it.
The direction of the axis of rotation found in this way is horizontal in Fig. 16; it is indeed parallel to the tilting axis of the specimen holder. We know from the way the grid was mounted, and taking into account electron optical image inversions, that the loop plane is inclined as represented in Fig. 16 by the two indications "up" and "down".

(ii) *Determination of the image side*

By comparing Fig. 16b and 16c which shows the same loops with a different sign for $\vec{g}$ (obtained by tilting) it is concluded that the image is inside on Fig. 16c for the indicated loops.

(iii) *Determination of the sign of* $\vec{s}$

The diffraction patterns corresponding to Fig. 16b and 16c show that $\vec{s}$ is positive in both cases. This is found to be invariably the case in the platinum foils. It is a consequence of the anomalous transmission which causes the rocking curve to be asymmetrical, having its maximum for positive s-values. Looking along the rotation axis from the left to the right of the photograph the diffraction spot producing contrast is to the right of the centre, when the contrast is inside the loop (Fig. 16b). With reference to Fig. 15b, which is drawn also viewed along the rotation axis in the same sense, one can conclude that the image is at the correct side only for vacancy loops (Fig. 14).

The procedure described here for one family of loops was repeated for several specimens and for several families of loops. It was found that both vacancy and interstitial loops are present. A similar conclusion was recently reached for loops in fission fragment irradiated aluminium [20]. Table I summarizes the results

of counting the number of identified loops. The statistics are not yet sufficient to draw a definite conclusion. Apparently the number of interstitial and vacancy loops seems to be roughly equal.

TABLE I

Number of experiment	Number of loops analysed	Loops of vacancy character	Loops of interstitial character
1	33	7	26
2	19	17	2
3	28	4	24
4	24	17	7
5	11	10	1

4.5. Loops with a stacking fault

Some of the loops in specimens, which were not used for the contrast experiments, apparently exhibit a uniform contrast inside. Although it is difficult to establish this definitely for loops of small size, some of the larger loops (see Fig. 12) also suggest that they exhibit stacking fault contrast. We will now show that this is not completely unexpected for interstitial loops. It is well known that the stacking fault in a loop resulting from the collapse of a single-layered vacancy disc can be removed by the passage of one partial of the type $\frac{a}{3}[11\bar{2}]$ [21]. The shear stress available for nucleating this partial is given by $\sigma = \gamma/b$.

The situation is, however, different for interstitial loops in the face centered cubic metals. An intrinsic stacking fault now results. This fault can be removed by the passage of two partials, one either side of the loop plane [22]. This is visualized in Fig. 18. After the first partial is nucleated the loop still contains a stacking fault (Fig. 18b) and its vector is of the type $\frac{a}{5}[141]$ resulting from the reaction $\frac{a}{3}[111] + \frac{a}{6}[\bar{1}2\bar{1}] \rightarrow \frac{a}{6}[141]$ [23]. No elastic energy is gained in this reaction. Since the fault is not eliminated completely, only a fraction of the stacking fault energy, say $\Delta\gamma_1$, is available for nucleating this first partial. The corresponding shear stress is $\sigma_1 = \Delta\gamma_1/b$. The shear stress available for nucleation of the second partial is then $\sigma_2 = (\gamma - \Delta\gamma_1)/b$.

The reaction taking place is now e.g. $\frac{a}{6}[141] + \frac{a}{6}[\bar{1}\bar{1}2] \rightarrow \frac{a}{2}[011]$. It may therefore well be that whereas stacking faults are readily removed from vacancy loops, they are not removed from interstitial loops in metals or alloys where the following relations are satisfied : $\sigma_c < \gamma/b$ but $\sigma_c > \frac{\Delta\gamma_1}{b}$ and $\sigma_c > \frac{\gamma - \gamma_1}{b}$ where σ_c is the critical shear stress necessary to nucleate the partial.

4.6. Conclusions

From the experiments described above and from the discussion the following conclusions can be drawn .

(i) The geometry of the crystal lattice is of importance if one wants to explain the details of damage formation . This is concluded from the decoration effects at subboundaries and at coherent twin boundaries .

(ii) The formation of loops seems to be a heterogeneous nucleation process . This is suggested by the influence of quenching on the concentration of loops and by the dependence of the concentration at a given dose on the damage rate .

(iii) The annealing behaviour of defects is influenced by the simultaneous presence of dissolved gases : the annealing temperature seems to be shifted upwards .

(iv) The irradiation with α-particles and with fission fragments produces as well vacancies as interstitials . Loops due to both types of defects can be identified and are observed after annealings at temperatures as high as 500°C .

(v) A technique is described in detail which allows in principle to determine the concentration of defects of each type by measuring the total area of loops .

REFERENCES

[1] GREENWOOD G.W., FOREMAN A.J., RIMMER D.E. : A.E.R.E. – R.1863 (1959)

[2] HIRSCH P.B., HORNE R.W., WHELAN M.J. : Phil. Mag. 1, 667 (1956)

[3] FISHER E.S. : Trans. AIME, 209, 882 (1957)

[4] HUDSON B., WESTMACOTT K.H., MAKIN M.J. : Phil. Mag. 7, 377 (1962)

[5] WHELAN M.J. : Vierter Int. Kongress für Elektronenmikroskopie, Berlin, 1958 (Springer Verlag, Berlin 1958) p.539

[6] HIRSCH P.B., SILCOX J., SMALLMANN R.E. and WESTMACOTT K.H. : Phil. Mag. 3, 897 (1958)

[7] SILCOX J. and HIRSCH P.B. : Phil. Mag. 4, 72 (1959)

[8] FRANK F.C. : Dislocations and mechanical properties of crystals (John Wiley & Sons, New York 1957) p.514

[9] SILCOX J. and HIRSCH P.B. : Phil. Mag. 4, 1356 (1959)

[10] BARNES R.S. and MAZEY D. : Phil. Mag. 5, 1247 (1960)

[11] RUEDL E., DELAVIGNETTE P. and AMELINCKX S. : J. Nucl. Mat. 6, 46 (1962)

[12] PIERCY G.R. : Phil. Mag. 5, 201 (1960)

[13] PASHLEY D.W. and PRESLAND A.E.B. : Proc. European Reg. Conf. on Electr. Micr. Delft 1960, p.391 (1961)

[14] SILSBEE R.H. : J. Appl. Phys. 28, 1246 (1957)

[15] LEHMANN C. and LEIBFRIED G. : Z. für Phys. 162, 103 (1961)

[16] THOMPSON M.W. : Phil. Mag. 4; 139 (1959) ; Proc. Roy. Soc., A 259, 458 (1961)

[17] GIBSON J.B., GOLAND A.N., MILGRAM M. and VINEYARD G. : Phys.Rev. 120, 1229 (1960)

[18] GROVES G.W. and KELLY A. : Phil. Mag. 6, 1527 (1961)

[19] SIEMS R., DELAVIGNETTE P. and AMELINCKX S. : Phys.Status Solidi 2, 421 (1962)

[20] WESTMACOTT K.H., ROBERTS A.C., BARNES R.S. : AERE-R 3946 (1962)

[21] KUHLMANN-WILSDORF D. : Phil. Mag. 3, 125 (1958)

[22] FRANK F.C. and NICHOLAS J.F. : Phil. Mag. 44, 1213 (1953)

[23] BARNES R.S. : Discussions of the Faraday Society, n° 31, 38 (1961)

[24] AMELINCKX S. et al. : Acta Met. 7, 8 (1959)

[25] PUGH S.F. : AERE-R – 3458 (1960)

[26] AMELINCKX S. : Phil. Mag. 3, 307 (1958)

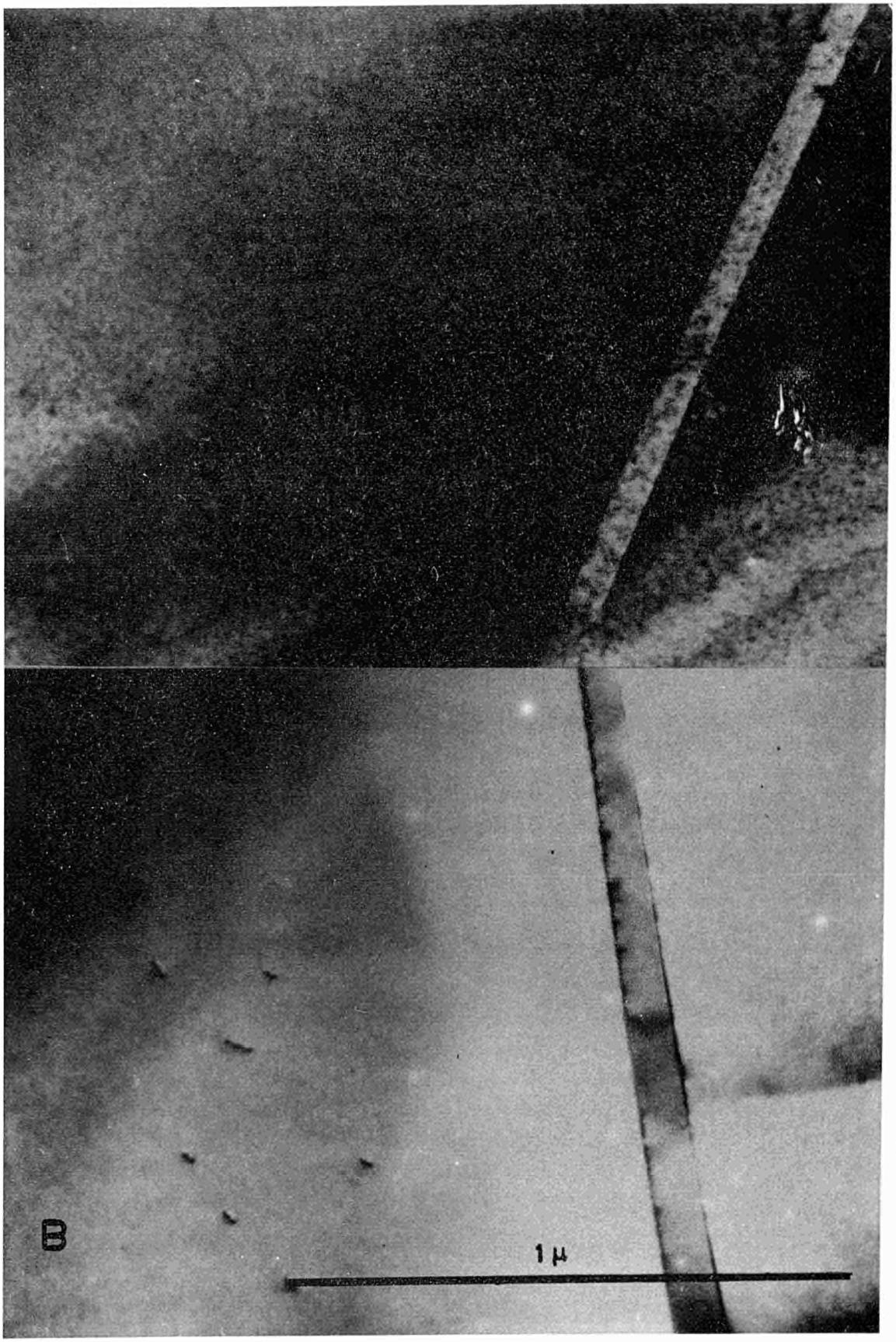

Fig. 1

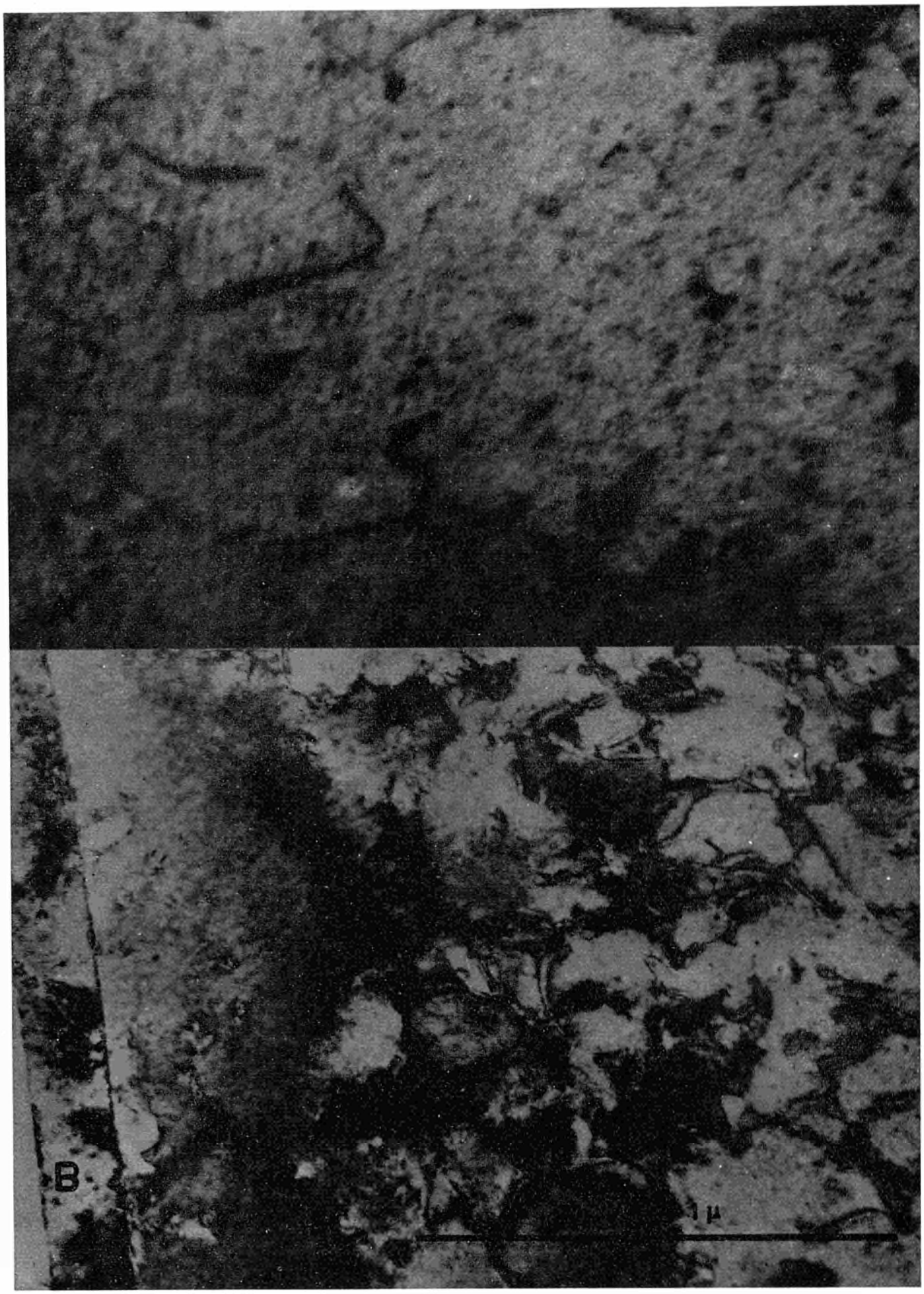

Fig. 2

C/195/63

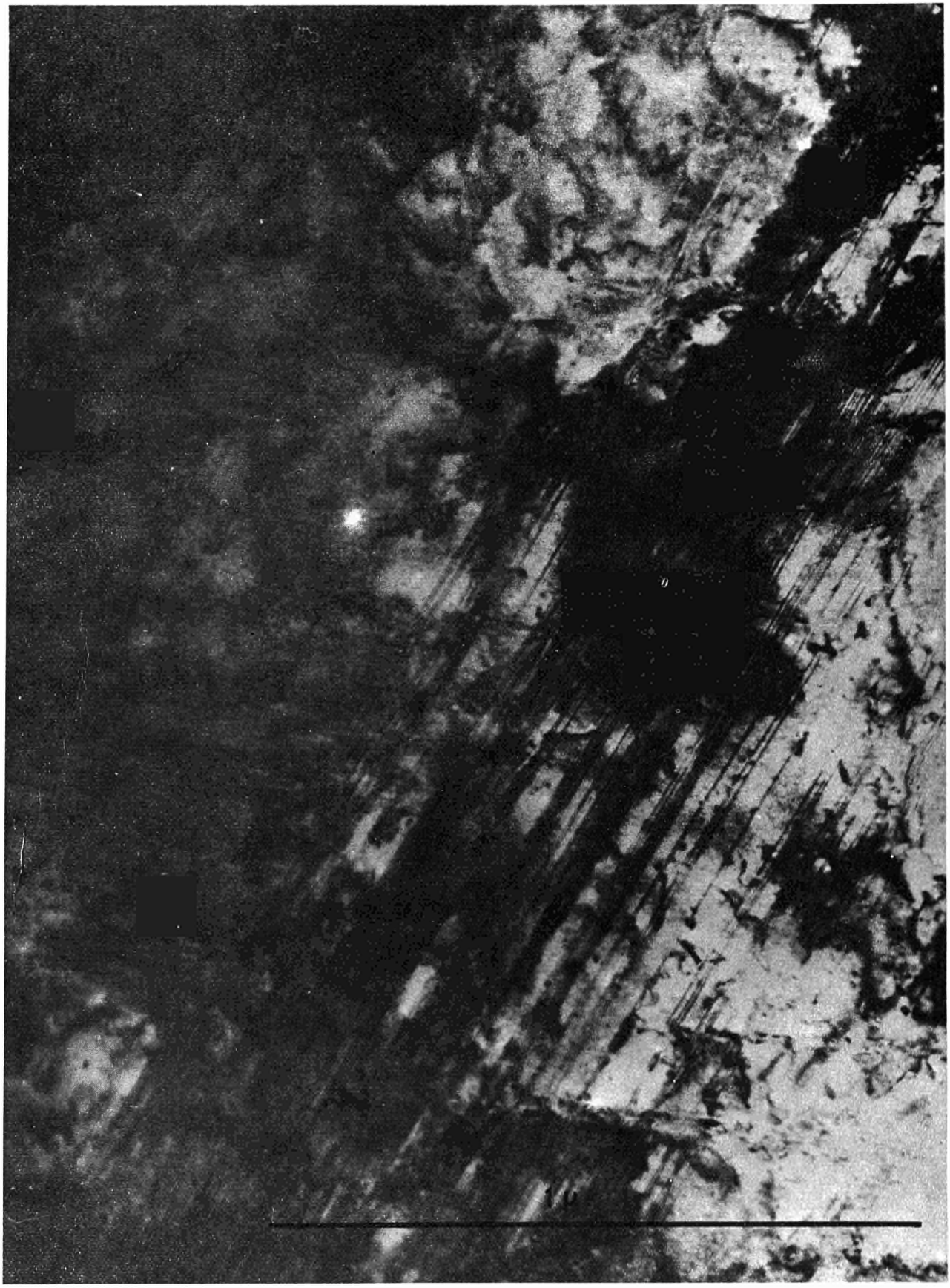

Fig. 3

C/195/63

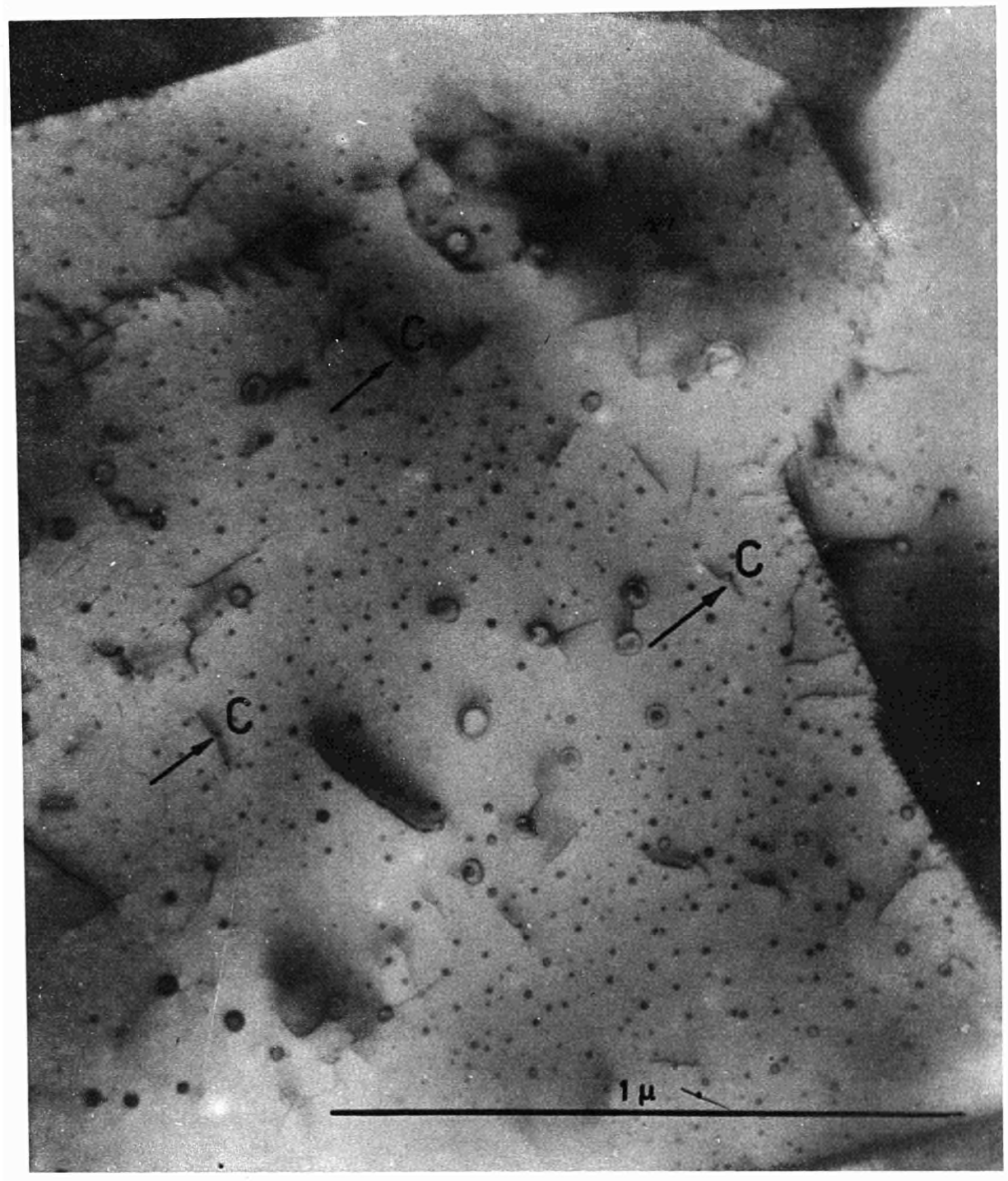

Fig. 4

Fig. 5

C/195/63

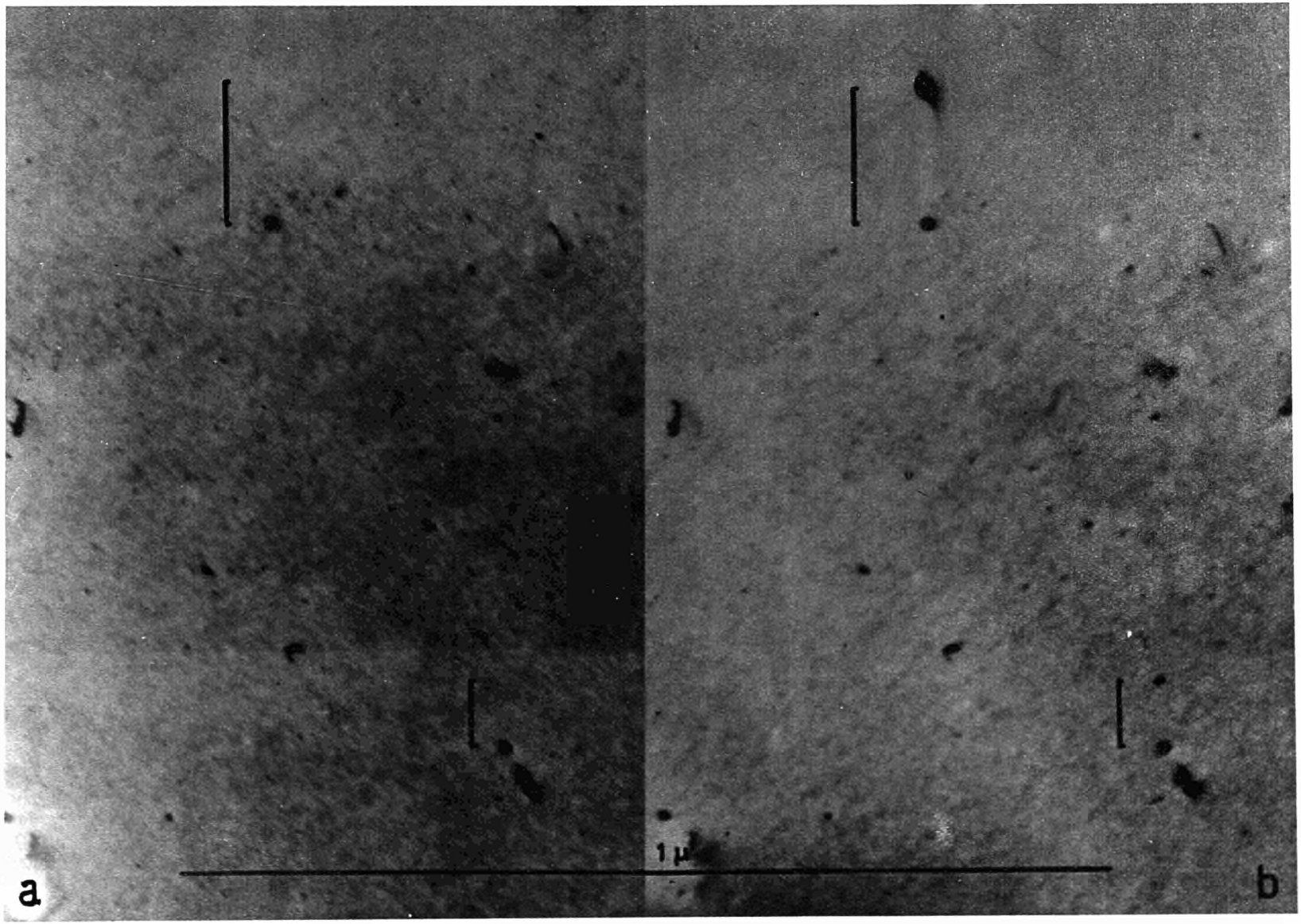

Fig. 6

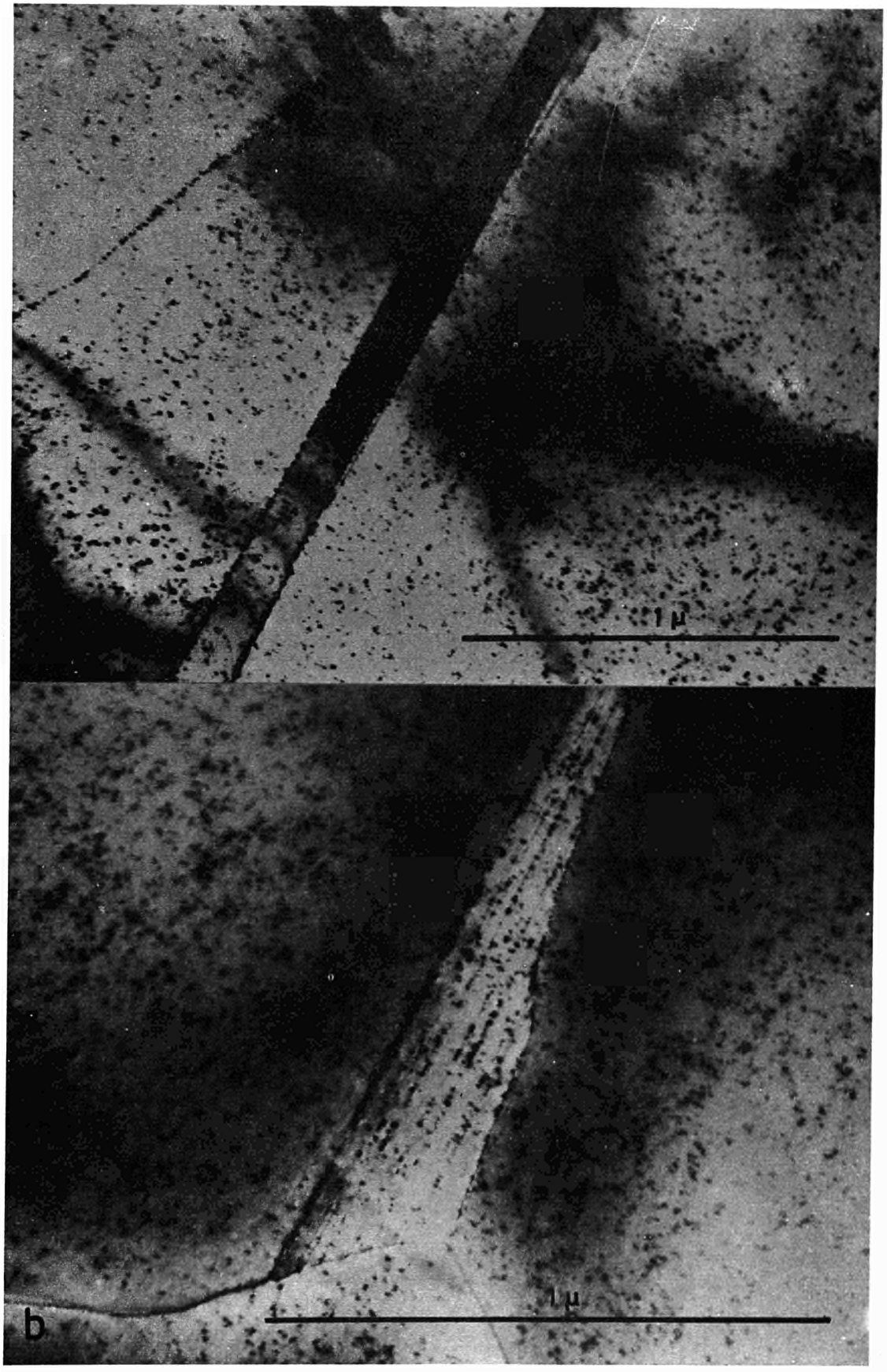

Fig. 7

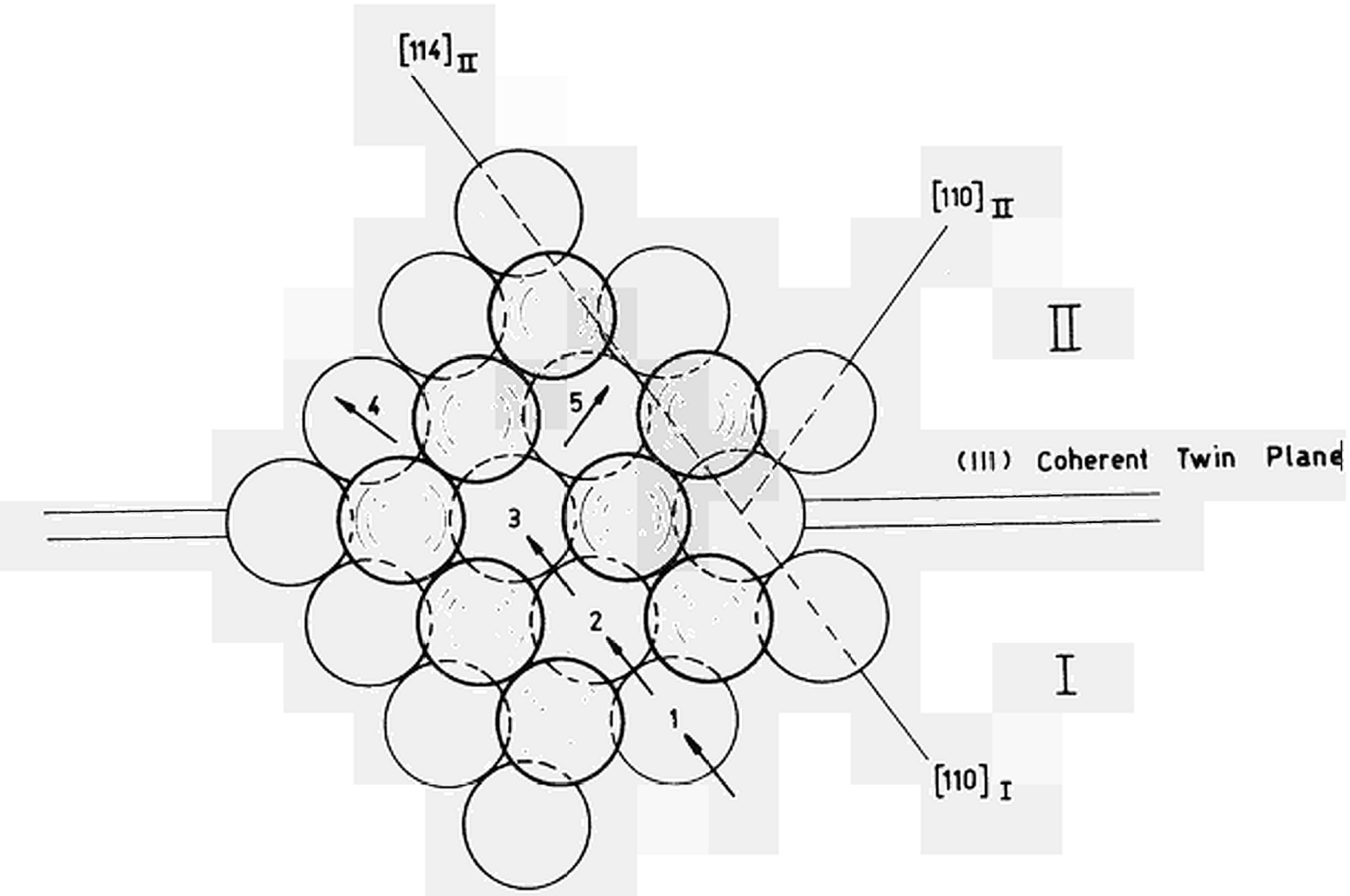

Fig. 8

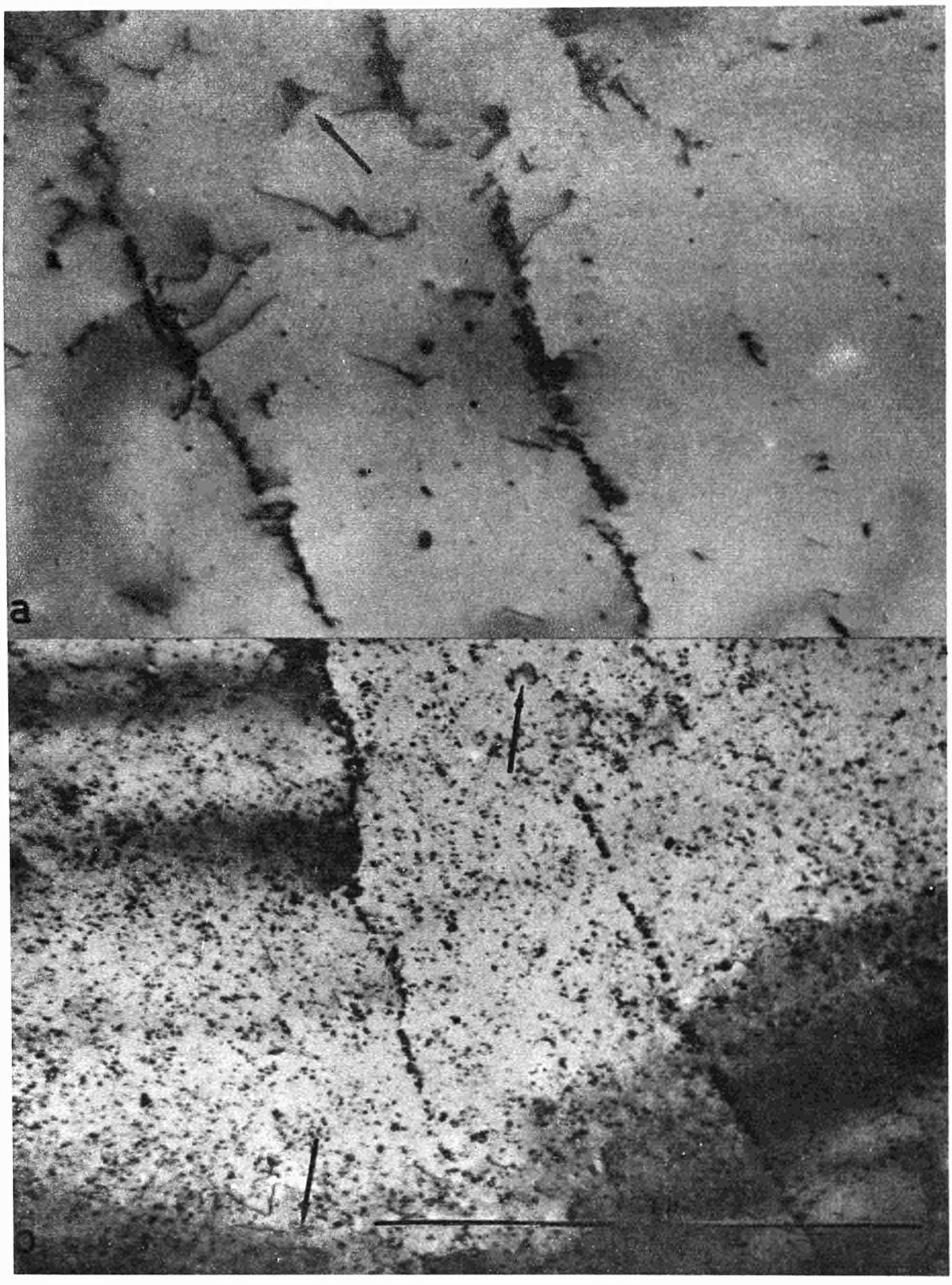

Fig. 9

Fig. 10

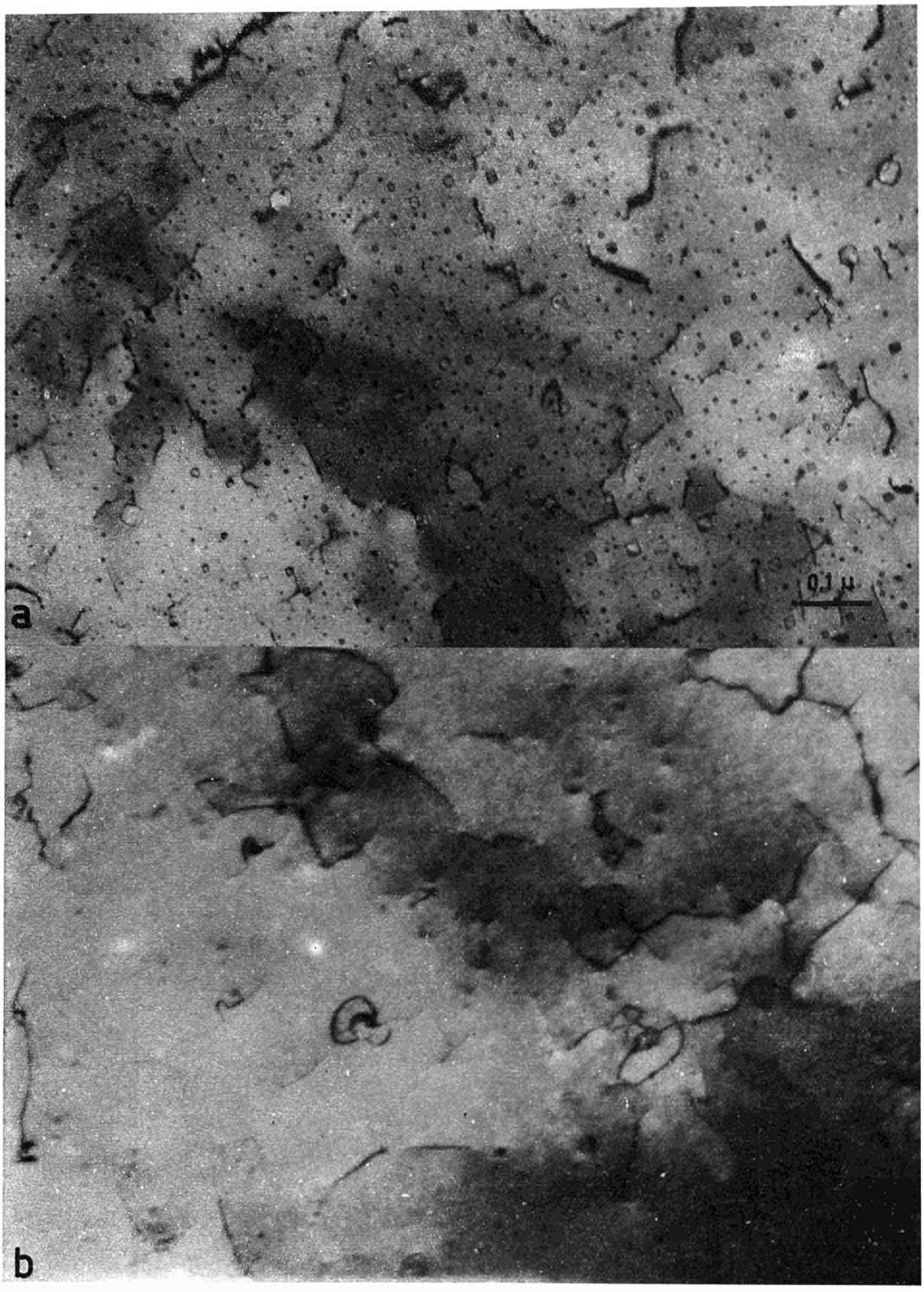

Fig. 11

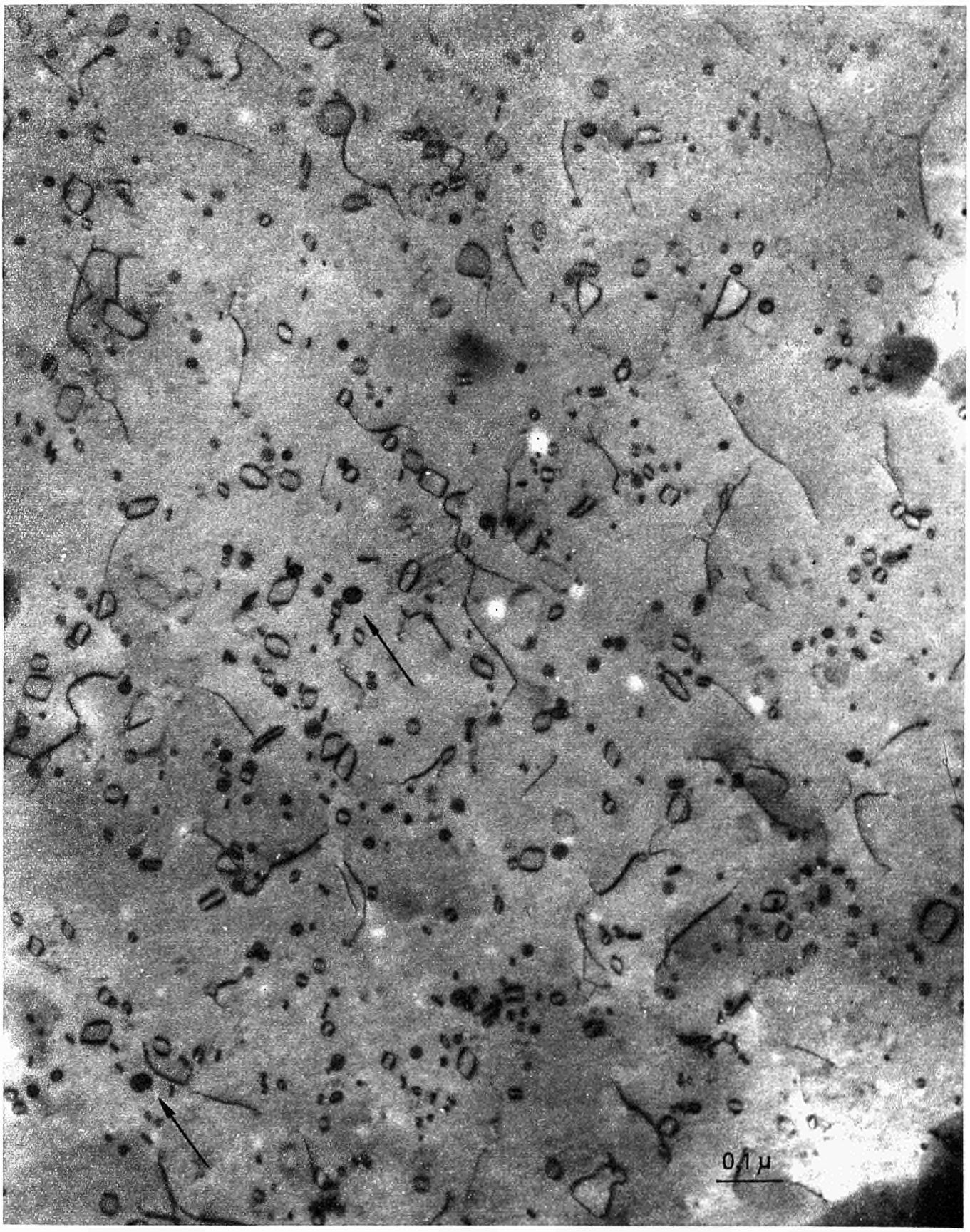

Fig. 12

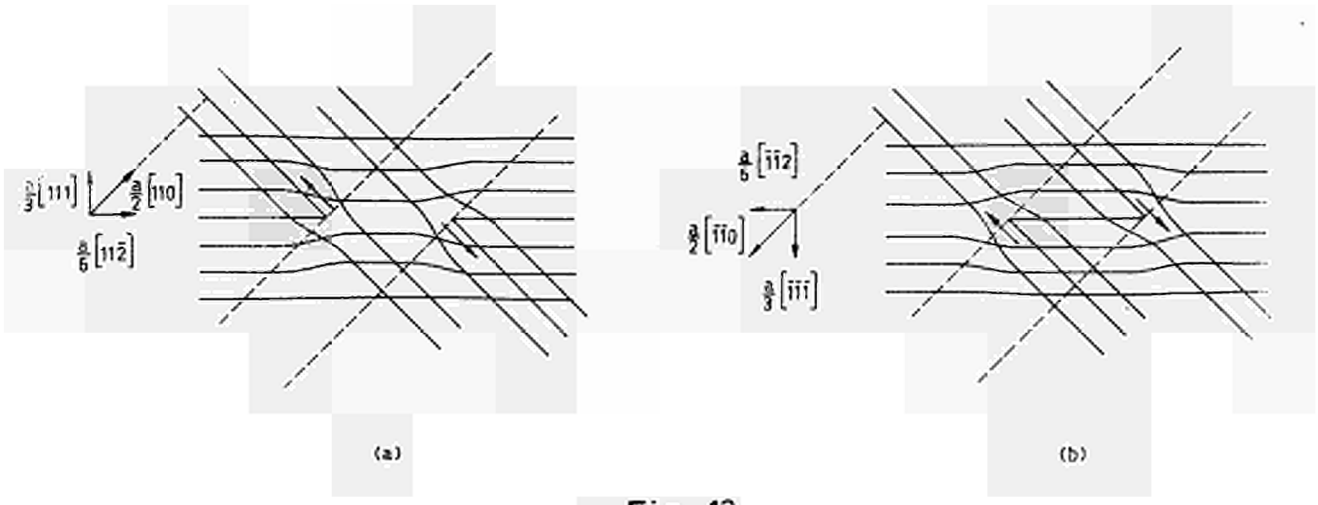
$\frac{a}{3}[111]$
$\frac{a}{2}[110]$
$\frac{a}{6}[11\bar{2}]$
(a)
$\frac{a}{6}[\bar{1}\bar{1}2]$
$\frac{a}{2}[\bar{1}\bar{1}0]$
$\frac{a}{3}[\bar{1}\bar{1}\bar{1}]$
(b)

Fig. 13

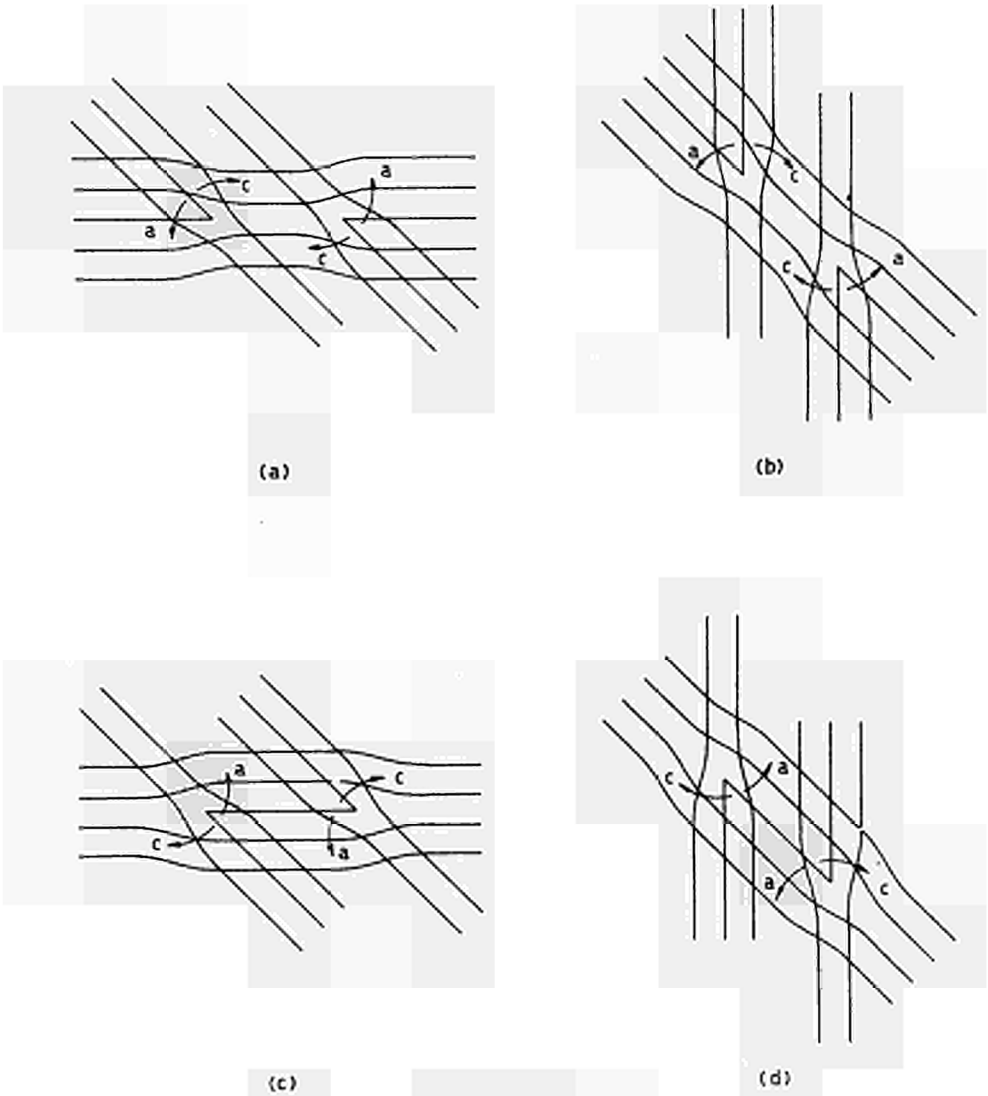
a
c
a
c
(a)
a
c
c
a
(b)
a
c
c
a
(c)
c
a
a
c
(d)

Fig. 14

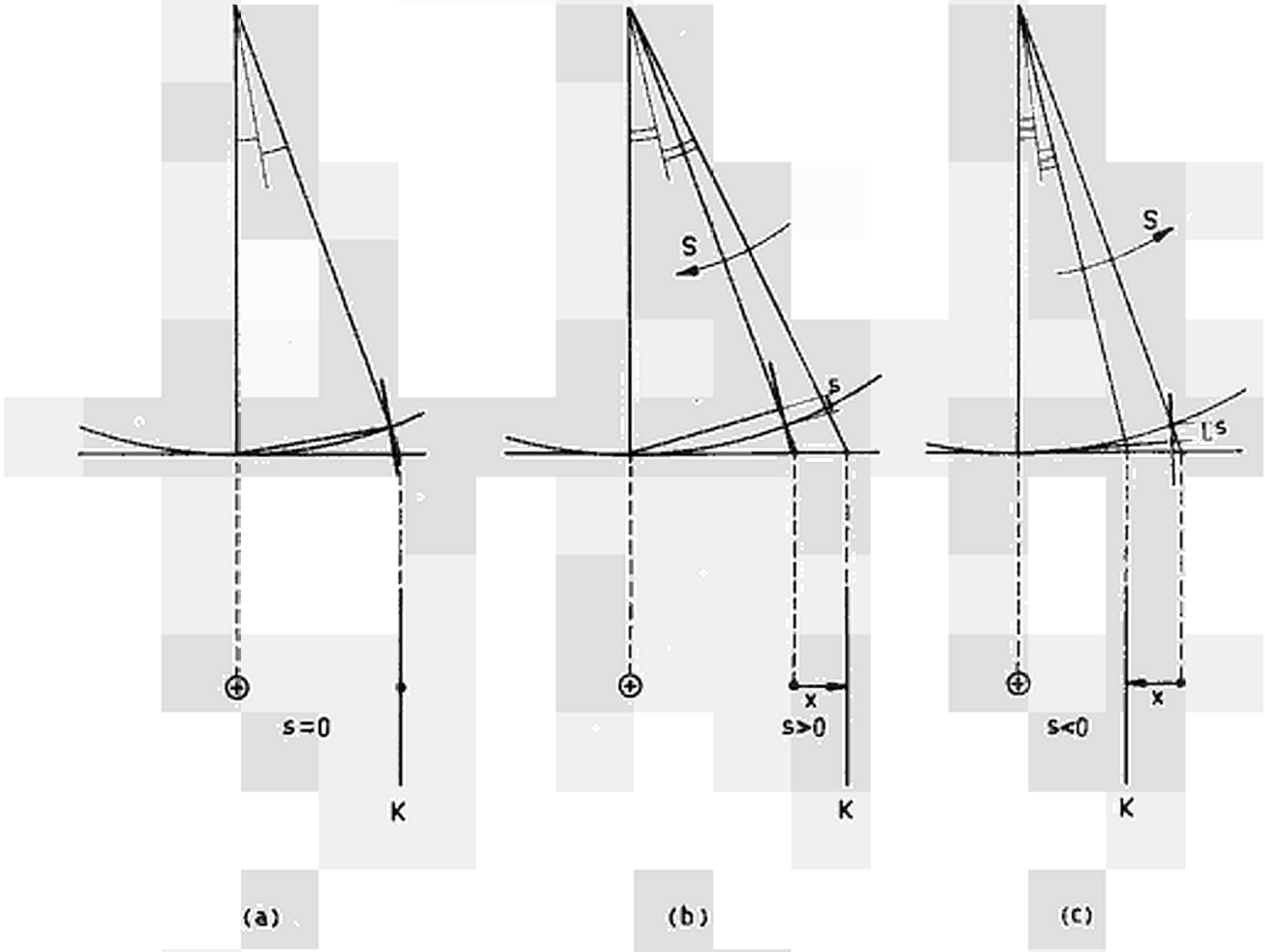

Fig. 15

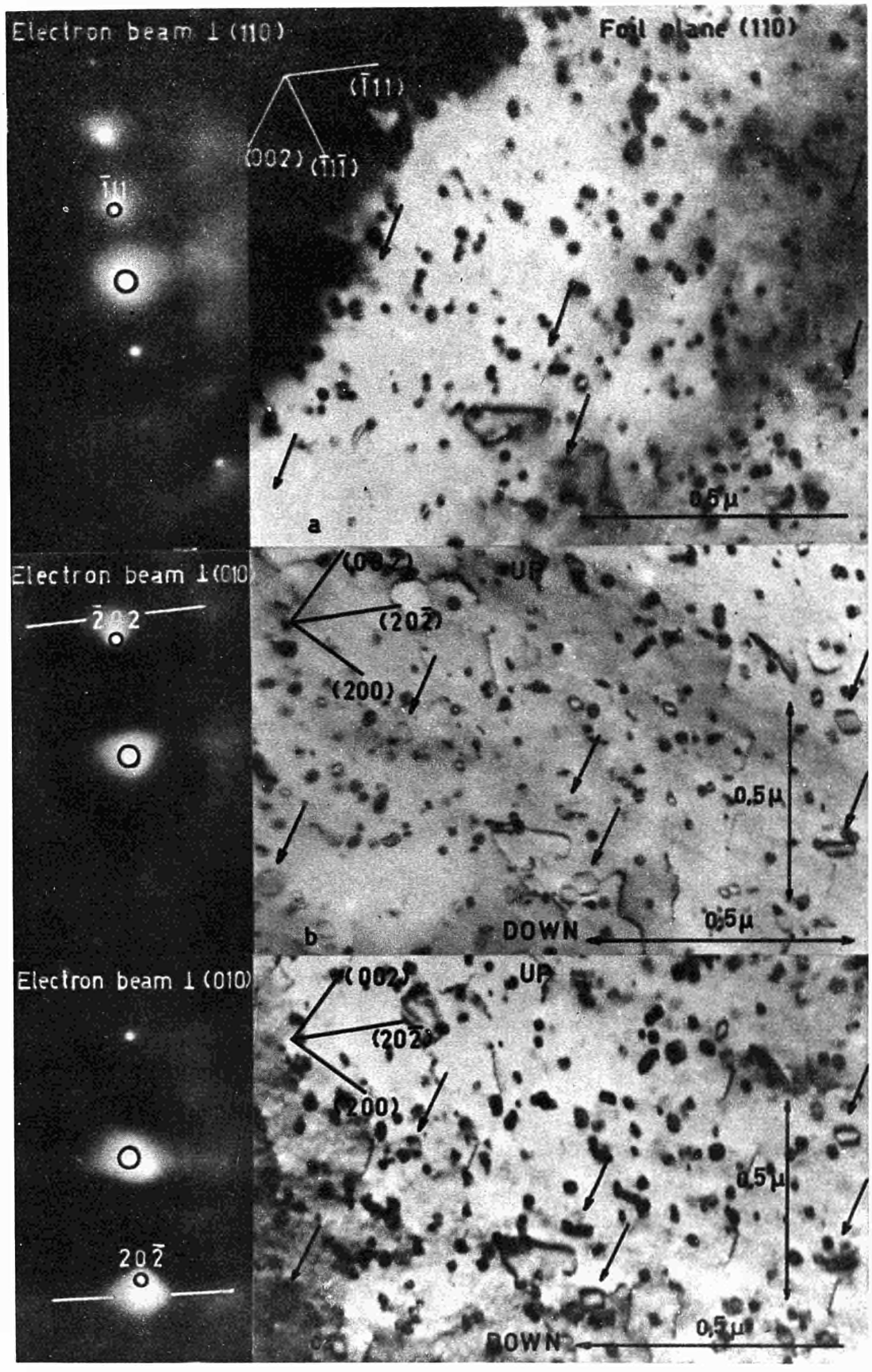
Electron beam ⊥ (110)
Foil plane (110)
(002)
a
0,5μ
Electron beam ⊥ (010)
UP
(200)
DOWN
b
Electron beam ⊥ (010)
UP
(200)
DOWN

Fig. 16

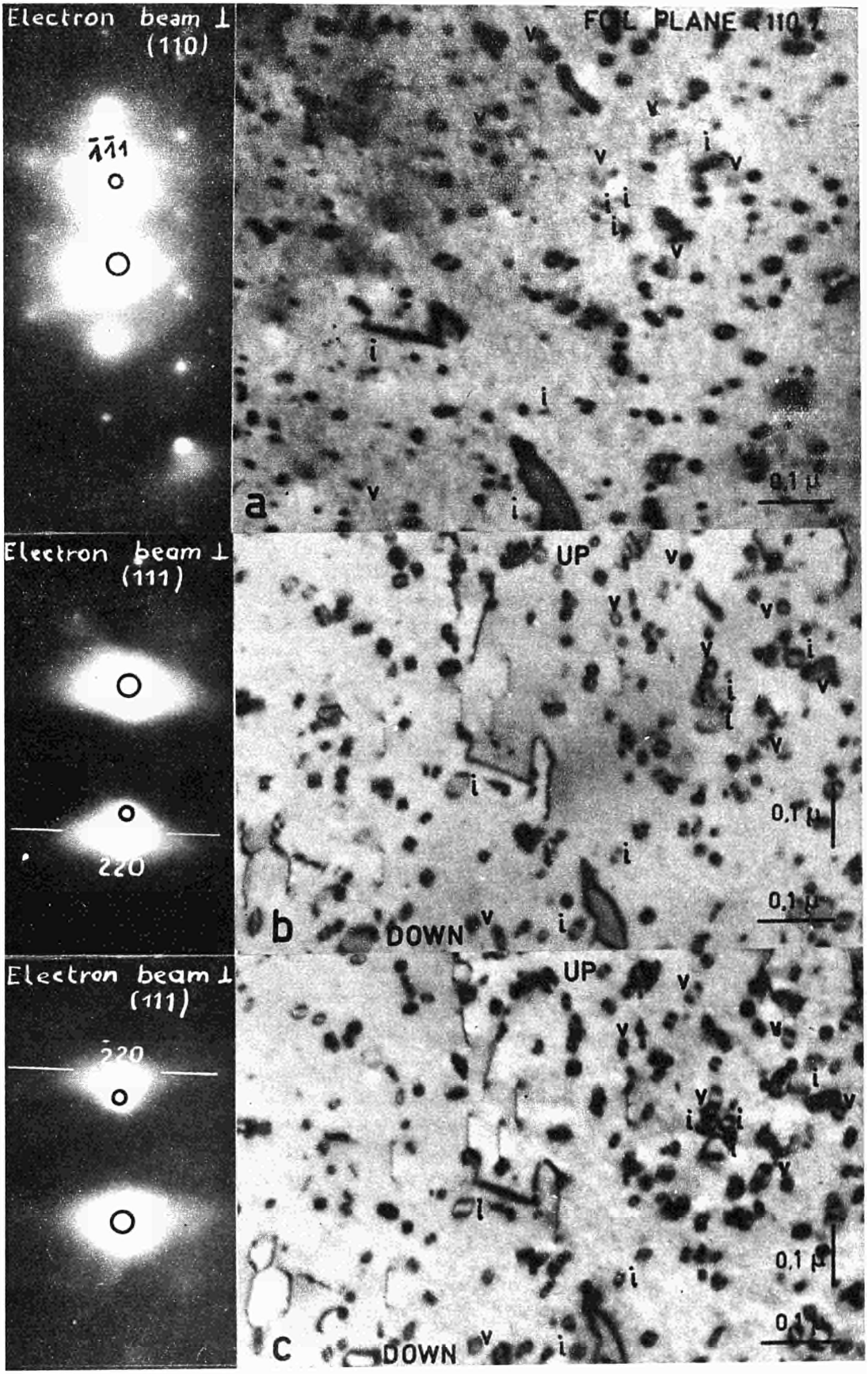

Fig. 17

C/195/63

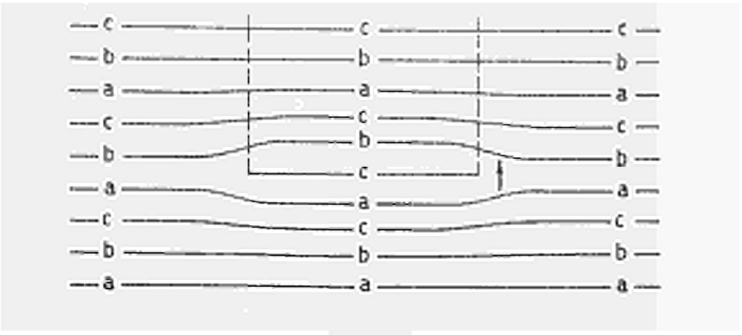
c
b
a
c
b
a
c
b
a
c
c
c
b
b
b
c
a
a
c
c
c
b
b
b
a
a
a
c
b
a
c
b
a
c
b
a
b
a
c
b
a
c
b
a
c
c
c
b
b
b
a
a
a
c
b
a
c
b
a
c
b
a
a
c
c
b
b
b
a
a
a

(a)

(b)

(c)

Fig. 18

CDNA00243ENC